Università degli Studi di Pisa
in collaboration with
Delft University of Technology
Process & Energy Department

Master of Science in
Mechanical Engineering

Rarefaction Shock Waves: a contribution to experiments and simulations

Thesis

Sergio Segreto

October 8, 2008

Supervisors:

Prof. P. Colonna

Prof. P. Di Marco

MSc. N. R. Nannan

Academic Year 2007 - 2008

Introduction

A shock wave is a thin region across which there is flow of matter such that in the direction of the flow, the substance experiences an abrupt change of state. As an exact result of the Euler equations, all fluid properties - pressure, velocity, density, etc. - are discontinuous across the shock, meaning that the state variation occurs in an infinitesimally thin region. The pressure jump is the thermodynamic property that characterizes a shock. If the pre-shock pressure is less than the post-shock pressure, the wave is named *compression shock wave* (CSW); conversely, if the pre-shock pressure is greater than the post-shock pressure, the wave is called a *rarefaction shock wave* (RSW).

According to the classical theory of gasdynamics, which is mostly based on the ideal gas equation of state (EoS), RSWs are inadmissible. Nevertheless, complex thermodynamic models show that compressible flows of fluids having a sufficiently large heat capacity may exhibit rarefaction shock waves, also referred to as nonclassical phenomena.

Apart from the numerous theoretical studies available in the scientific literature, no experimental evidence of RSWs in the dense vapor thermodynamic region is, however, currently available. In order to prove their existence, a new facility has been built at the P&E Department of the Delft University of Technology. The present work mainly aims at contributing to the commissioning of the shock tube. An attempt is made to provide insight into the flow field that the experimenter may generate in shock tube facility. For this purpose a CFD solver, namely *Fluent*, is used, together with a real gas EoS, to simulate experimental runs.

Theoretical Aspects of BZT Effects in Dense Gases

In dense gases with large isochoric specific heat capacity C_v, the isentropes tend to superimpose upon the isotherms in a (v, p) thermodynamic plane because

$$C_v \to \infty \Rightarrow \left.\frac{\partial p}{\partial v}\right|_s = \left.\frac{\partial p}{\partial v}\right|_T - \frac{T}{C_v}\left.\frac{\partial p}{\partial T}\right|_v^2 \to \left.\frac{\partial p}{\partial v}\right|_T \tag{1}$$

where p is the pressure, T is the temperature, v the specific volume and s the entropy. This shows that in a limited region close to the critical point, where the isotherms of all fluids must have a downward curvature, the isentropes of fluids of sufficient molecular complexity display two inflection points which bound a region of negative concavity.

A nondimensional measure of the curvature of the isentropes in the (v, p) thermodynamic plane is given by the fundamental

derivative of gasdynamics, defined as

$$\Gamma \equiv 1 + \frac{\rho}{c}\frac{\partial c}{\partial \rho}\bigg|_s = -\frac{v}{2}\frac{\dfrac{\partial^2 p}{\partial v^2}\bigg|_s}{\dfrac{\partial p}{\partial v}\bigg|_s}, \qquad (2)$$

with ρ the density and c the adiabatic speed of sound.

Γ determines the qualitative behavior of compressible flows. Since the denominator

$$\frac{\partial p}{\partial v}\bigg|_T \leq 0$$

everywhere from the requirement of thermodynamic stability, then

$$\frac{\partial^2 p}{\partial v^2}\bigg|_s > 0 \;\Leftrightarrow\; \Gamma > 0$$

which is valid, for example, for gases far from the critical point, while

$$\frac{\partial^2 p}{\partial v^2}\bigg|_s < 0 \;\Leftrightarrow\; \Gamma < 0$$

which is instead valid for dense gases near the critical point. Therefore, in the finite region of negative curvature of the isentropes, the value of Γ is negative. Because of the pioneering work of Bethe, Zel'dovich and Thompson in the field of nonclassical gasdynamics, a fluid that exhibits a $\Gamma < 0$ region in the vapor phase is referred to as a *BZT fluid*. The *BZT region* is delimited, for a single-phase fluid, by the dew line and the $\Gamma = 0$ locus, which represents the locus of the points where the isentropes change their curvature, as shown in figure 1.

Equation 2 also shows that the sign of Γ influences the variation of the sound speed with density. In the region where $\Gamma < 1$, the speed of sound exhibits unusual behavior, because its value increases over isentropic expansions and decreases over isentropic compressions. This reverted trend could lead to the formation of RSWs, as shown by the balance equations applied to disturbance waves and solved via the method of characteristics.

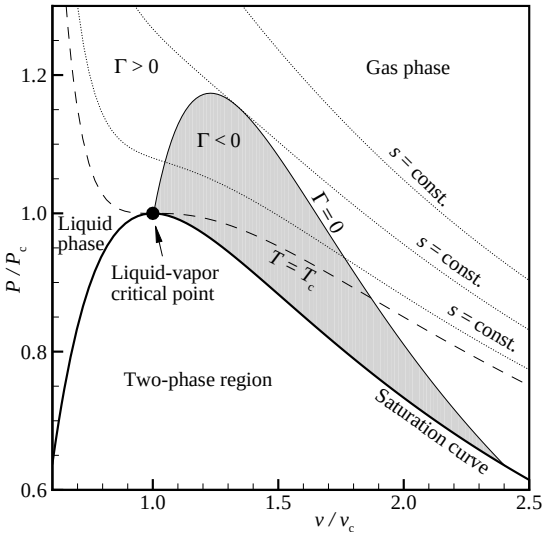

Figure 1: Liquid-vapor saturation curve and $\Gamma < 0$ region (shaded region) for a BZT fluid. Thermodynamic properties are from the van der Waals EoS.

Neglecting the body forces acting on the fluid, and assuming that the flow is confined to a one-dimensional duct of constant cross-sectional area, so that all variables of interest depend only on x and t, and moreover that the flow is homentropic, the continuity and the momentum equations can be combined to

yield

$$\left[\frac{\partial}{\partial t} + (U \pm c)\frac{\partial}{\partial x}\right](U \pm F) = 0, \tag{3}$$

where U is the absolute velocity of a fluid particle. The terms $U + c$ and $U - c$ are the velocities of waves travelling in the positive and negative direction, respectively. The paths tracked by the waves appear as lines on the (x, t) diagram. Such lines are called characteristics. The quantities $U + F$ and $U - F$ do not vary along their respective characteristic. For an observer moving, for example, with one positive wave, the quantity $U + F$ does not change in time, though it changes from one characteristic to another. If the disturbance waves travel toward a region of uniform flow, the characteristics are straight lines. In general, the characteristics will not be parallel but will either converge or diverge in the moving perturbed region; where they first intersect, a shock forms. By introducing the fundamental derivative, the variation of the speed of positive waves along one negative characteristic line is

$$d(U + c) = \Gamma dF = \frac{\Gamma}{\rho c} dp. \tag{4}$$

Therefore a shock moving in the positive x direction forms if $d(U+c) > 0$. Thus if $\Gamma > 0 \rightarrow dp > 0$, i.e., compressive disturbance waves will steepen to form a shock (as in the case of the perfect gas), and if $\Gamma < 0 \rightarrow dp < 0$, e.g., expansive disturbances will steepen to form a shock. Finally, if the hypothetical case of $\Gamma = 0$ is considered, then the characteristics will be parallel and the waves will proceed undistorted.

Once the shock is formed, the method of characteristic cannot be used to link pre- and the post-shock thermodynamic states, since the flow becomes nonhomentropic. The conservation equations for mass, momentum and energy can be applied to a control volume that surrounds the shock wave and that moves at a constant speed with it. Under the assumptions of quasi one-dimensional, inviscid, adiabatic flow, and neglecting body forces, mass diffusion and heat generation, the jump relations linking the two states, namely the pre-shock state 1 and the post-shock state 2, also known as the Hugoniot-Rankine relations, are

$$\begin{aligned} \rho_1 u_1 &= \rho_2 u_2 \\ p_1 + \rho_1 u_1^2 &= p_2 + \rho_2 u_2^2 \\ h_2(p_2, v_2) - h_1(p_1, v_1) &= \frac{1}{2}(p_2 - p_1)(v_1 + v_2). \end{aligned} \tag{5}$$

In addition, from the second law of thermodynamic,

$$s_2 - s_1 \geq 0. \tag{6}$$

Equation 6 is referred to as the entropy admissibility condition. Moreover, from mathematical considerations on the shock equations,

$$M_1^r \geq 1 \geq M_2^r \tag{7}$$

where M^r is the Mach number relative to an observer moving with the shock. Equation 7 is referred to as the mechanical stability condition. Equations 6 and 7 pose restrictions to all the possible sets of upstream and

downstream states which satisfy the conservation equations. Equation 7 states that the upstream flow relative to the shock is (super)sonic, while the downstream flow relative to the shock is (sub)sonic.

An alternative way to show the possibility of creating RSWs follows from the entropy condition 6. The relationship between the entropy change and the pressure jump across a weak shock is

$$\Delta s = \frac{1}{6}\,\Gamma_1\,\frac{v_1^3}{T_1\,c_1^4}\,(p_2 - p_1)^3 + O\,(p_2 - p_1)^4\,. \quad (8)$$

The weak shock theory therefore identifies compressive ($\Delta p > 0$) shocks as physically admissible shocks ($\Delta s > 0$) if $\Gamma_1 > 0$, whereas rarefaction shock waves ($\Delta p < 0$) can occur only if $\Gamma_1 < 0$. This implies that expansion waves will spread into fans and compression waves will steepen into shocks if the fundamental derivative Γ_1 is positive, and that expansion waves will steepen into shocks and compression waves will spread into fans, that is, the reverse behavior of classical flows, when the fundamental derivative Γ_1 is negative, in agreement with what is found via the method of characteristics.

Nonclassical gasdynamic effects can occur in a flow field if the ratio of the universal gas constant and the isochoric specific heat, i.e., $\delta = \dfrac{R}{C_v}$ is small enough, depending on the equation of state used. Nevertheless, if nonclassical gasdynamics is to be proven, other important considerations which need to be taken into account are the availability of thermophysical property data, fluid characteristics, e.g., thermal decomposition temperature, fluid availability and price, and safety concerns such as toxicity and flammability. Currently three classes of fluids are believed to exhibit a BZT region in the vapor phase, namely, hydrocarbons, perfluorocarbons, and siloxanes.

Siloxanes are a family of fluids composed of complex molecules containing alternate silicon and oxygen atoms in either a linear or cyclic arrangement. Two or three methyl groups CH_3 are usually attached to each silicon atom. The Span and Wagner equation of state, used in this work to model the thermophysical properties of the cyclic molecule D_6 (dodecamethylcycloexasiloxane), is the most up to date equation for this family of fluids.

Due to their nontoxicity, excellent thermal and chemical stability, and limited flammability, siloxanes are possibly the most suitable fluids from an engineering point of view. An added benefit of siloxanes is that these substances are already employed as working fluids in oganic Rankine cycle engines (ORCs) and are proposed for promising ORC applications. The isentropic efficiency of these turbines can in principle increase if they are operated with fluids that exhibit nonclassical behavior, and if the expansion process is carried out, even partially, in the nonclassical gasdynamic region.

Commissioning of the Flexible Asymmetric Shock Tube (FAST)

The FAST is a shock tube whose goal is to generate and detect an RSW. In the way it operates, shown in figure 2, it is similar to a Ludwieg tube, i.e., a shock tube able to generate short duration steady supersonic flows.

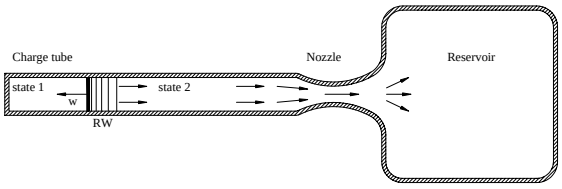

Figure 2: Schematic representation of the FAST, showing the main components and the propagation of a rarefaction wave into the charge tube.

A 9 *m* long duct of constant cross-sectional area, named charge tube (CT), is connected, via a fast-opening valve (FOV), to a low-pressure plenum (LPP). If the high-pressure and the low-pressure initial thermodynamic states are properly chosen, the fast opening (4 *ms*) of the valve initiates a flow consisting of compression waves moving into the LPP and of expansion waves that will in principle coalesce in the CT to form an RSW. Due to the peculiar shape of the FOV, a convergent-divergent nozzle is present between the tube and the reservoir. Since the RSW induces a steady subsonic flow at the inlet of the nozzle, the flow is accelerated to supersonic velocity. Therefore, choked sonic conditions are set at the nozzle throat, this way avoiding that disturbances arising in the LPP propagate into the CT disturbing the shock formation.

Figure 3: View of the Flexible Asymmetric Shock Tube.

Four dynamic pressure instruments, which can detect the passing wave, are placed along the tube, two of them at half of the pipe length, and other two toward the end of the charge tube. The estimate of the speed of the wave is then made possible by correlating their signals, if their relative distance is exactly known.

The initial thermodynamic states are carefully chosen in order to maximize the relative Mach number $M_{upstream}$. An appropriate control system helps realizing the experimental conditions. The control logic used to reach those stable initial states (p and T) of the working fluid inside the charge tube and the low-pressure plenum is implemented using the software *LabView*. The control system

has been conceived with four cascaded control loops:

1. HFT control loop

The experiment has to be conducted in the vapor phase at high ($\approx$ 370 $^{\circ}C$) temperature. Therefore, a heating tank (HFT) provides the experimental section of the setup with the dense vapor. The first control loop regulates the electrical heater of the HFT such that the saturation vapor pressure measured by a static pressure sensor in the HFT is uqual to a preset pressure.

2. RT control loop

Before reaching the charge tube, the saturated vapor flows inside a reference tube (RT), whose task is to provide the thermocouple used to thermostate the CT with a reference value. As the initial state must be slightly superheated, the second control loop, shown in figure 4, compares the saturation temperature, as measured by the temperature sensor placed in the HFT, to the temperature measured by the temperature sensor in the RT. The controller regulates the electrical heaters of the RT such that the overheating is equal to a specified value.

3. CT control loop

The third control loop utilizes the temperature provided by the RT as reference temperature for the heating of the CT. Differential thermocouples, of which one end is placed on the RT and the other end on the CT, underneath the electrical heaters, provide with a temperature difference between the RT and the CT. The controller then regulates the measured temperature difference to the desired value acting on the electrical power of the heating elements.

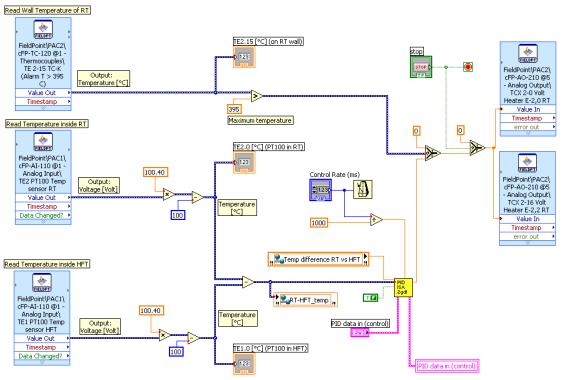

Figure 4: Representative LabView control loop block scheme.

4. LPP control loop

The fourth control loop regulates the gas temperature inside the LPP, measured by a temperature sensor, in order to obtain the same temperature as in the CT.

Moreover, LabView allows for the monitoring of most of the signals and for the semi-automation of all the procedures that the operator has to follow to properly set up the test run.

The monitoring is accomplished via a set of so-called Virtual Instruments (VIs) which provide the operator with the real time trends displayed in a user-friendly graphical interface.

A detailed description of the sequence of operations that any operator has to follow, in order to run an experiment, has been carefully conceived. The supervisory software also provides guidance to follow these procedures by means of series of dialog boxes.

Unsteady Simulation of the RSW Formation during the Opening of the Valve: an Eulerian approach with a sliding mesh

Various simulations employing siloxane D_6 as working fluid have been performed. Firstly, the simple nonclassical shock tube problem has been solved. Secondly, the flow through a simplified geometry has been simulated, by assuming the instantaneous opening of the valve. However, the finite opening time of the valve, the steep variation of the cross-sectional area through the nozzle of the real FOV, and the change of direction felt by the fluid moving from the CT toward the LPP, do in fact occur in the experiment and could significantly modify the previous numerical results.

Facing the problem from a theoretical point of view, the method of characteristics allows for the computation of the distance (either in space or in time) from the valve location at which the RSW forms, thus taking into account the effects of the finite opening time of the valve. The travelling speed of disturbance waves, which acts on the shock formation, can be theoretically computed by means of the conservation equations applied to a steady isentropic flow through a duct of varying cross-sectional area.

During the opening of the valve, an unsteady flow field arises, since the fluid is accelerated from rest conditions as long as the initial expansion waves propagate into the CT. This leads to departure from the theoretical case. As a consequence, the theoretical thermodynamic state downstream of the shock as well as the distance at which the shock fully forms might change. Therefore, to qualitatively predict the flow field, a CFD simulation is indeed necessary.

Modelling of the setup

The geometry of the facility is modelled taking into account the presence of the fast-opening valve. Thus, the geometric model is a rather accurate representation of the FAST. With reference to a cylindrical coordinate system, since geometry, constraints and initial conditions do not depend on the angular coordinate, the problem can be approximate as axisymmetric; therefore, only half of the axial section of the pipe is modelled. The grid discretizes the model in 2739 cells. The mesh is mapped and composed of quadrilateral elements in the CT, while triangular cells pave the LPP and the

FOV, as shown in figure 5. Before the opening of the valve, the fluid is at rest and at steady thermodynamic conditions, in both the high-pressure side (CT) and the low-pressure side (LPP). The initial thermodynamic states of the fluid are the same that will be set for the experiment. In order to simulate the opening of the valve, the grid is divided into two domains. The domain modeling the LPP entirely slides. The duct is considered as a closed system surrounded by adiabatic walls. The boundary condition employed to model the sliding part of the valve in both the reservoir and the charge tube is such that it behaves as a wall if the grid of the two domains does not overlap and as an open gap where the interfaces do overlap. The unsteady balance equations are solved, by means of an implicit numerical method, employing a constant time step of 10^{-7} s. The numerical schemes adopt second order derivative in both space and time.

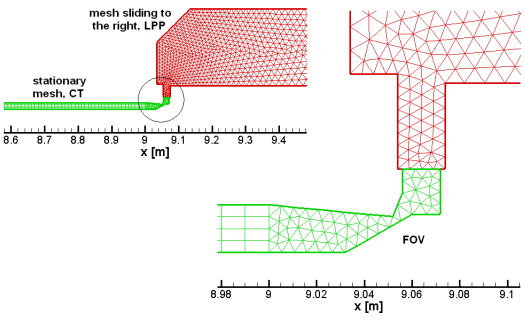

Figure 5: Cross-sectional area and grid topology, with the geometric details of the FOV. The two domains are represented using different colors.

Numerical results

Figure 6 represents the pressure contour during the opening of the valve at different times. Notice that the fluid is subject to a change of direction moving toward the low pressure side, and this reflects in a distortion of the travelling waves behind the nozzle throat. Moreover, the plots show that the waves, separated by initially different distances, are almost equi-spaced at the throat. To better understand this behaviour, the travelling speed of the waves is computed. The resulting plot is reported in figure 7. Despite the mesh, which is made up of only 6 elements along the nozzle axis, two main features can be noticed. Firstly, the travelling speed of the waves is the same at the throat, even if the local pressure changes, since sonic conditions are not

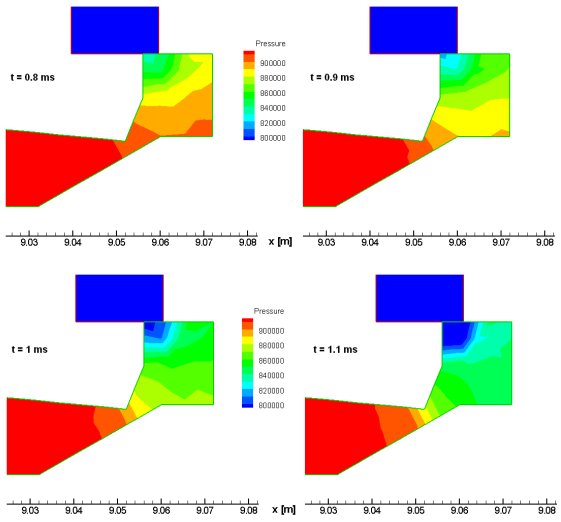

Figure 6: Pressure contour at different times during the opening of the valve.

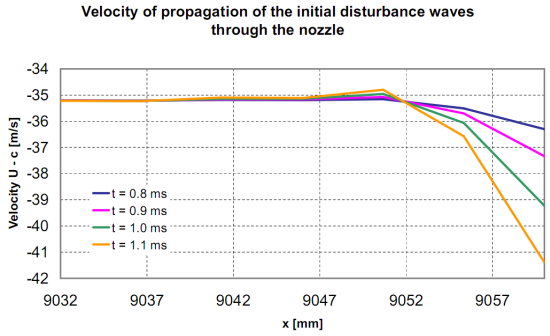

Figure 7: Sound speed along the nozzle centerline at different time steps during the opening of the valve.

formed yet at the throat. Secondly, the velocity of propagation of the waves behind the throat increases in time at a fixed location, as the expansion process takes place in the convergent-divergent nozzle, and it decreases approaching the throat.

1 *ms* after having started the opening of the valve, the first disturbance wave is already located in the convergent part of the nozzle; the flow accelerates toward the nozzle throat, but it slows down in the divergent part, as the absolute Mach number $M < 1$. As long as the head of the expansion process moves forward inside the CT, the pressure at the nozzle throat decreases until it reaches a stable value, corresponding to $M = 1$. After 2.5 *ms* the open gap has no more influence on the formation of disturbance waves, since the thermodynamic state at the interface between the charge tube and the reservoir is already set. The nozzle has already reached the steady sonic condition at the throat, therefore the flow is choked.

As displayed in figure 8, disturbances that occur downstream of the throat do not propagate into the charge tube. Notice that the presence of the nozzle helps the formation of a rarefaction shock, as it is already formed - although without a steady thermodynamic state behind it - after ≈ 4 *ms*.

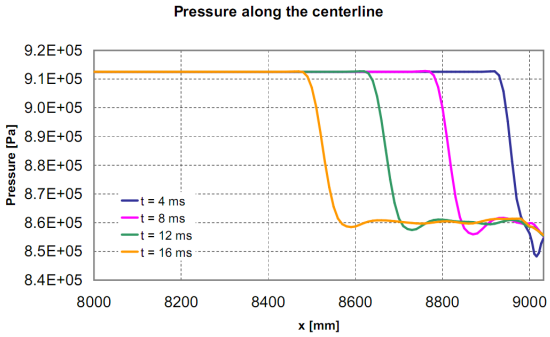

Figure 8: Pressure distribution along the centerline at different time steps.

The travelling wave is believed to be a rarefaction shock since both the entropy condition and the mechanical stability condition are satisfied. Nevertheless, the downstream state is different from the theoretical thermodynamic state.

Even though transport phenomena are neglected, the shock is not simulated as a discontinuity, but it is spread over different cells $(4 - 6)$, therefore showing a continuum structure. This also depends on the mesh size. In figure 9 the speed of sound distribution along the centerline is plotted for different instants. The sound speed increases during the isentropic expansion process in the nozzle. It is remarkable that even though disturbances

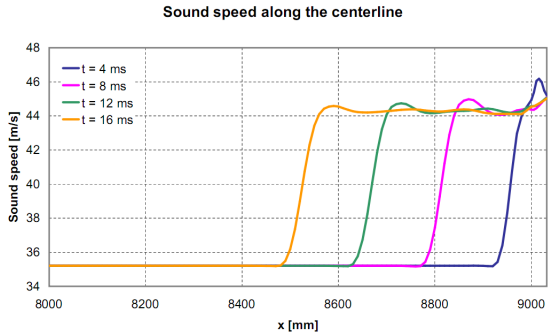

Figure 9: Speed of sound profile along the centerline at different time steps.

are present inside the reservoir, the numerical solution ahead of the nozzle throat is independent of them.

Conclusions and Recommendations

The FAST setup is at present under commissioning. Pressure safety tests and heating tests have already been performed. Moreover, in order to check the algorithm that allows for the cross-correlation among the signals coming from the dynamic pressure sensors, compression shock waves have been generated and measures performed inside the charge tube, using air at ambient temperature as working media. Leakage tests and tests with siloxane still need to be done, prior to the true experiments using siloxanes.

The performed simulations show two unexpected results: firstly, the presence of the nozzle, designed in order to avoid propagation of disturbances from the LPP toward the CT, seems to help the formation of an RSW because the distance from the valve interface at which the shock forms is reduced; secondly, the steady thermodynamic state set by the shock differs from the theoretical one. Note that these interesting results have been achieved using a rather coarse mesh, a grid sensitivity study has not been performed yet, due to the long computational time required for the simulation. Furthermore, transport phenomena related to viscosity have been neglected, even though theoretical computations of the Reynolds number along the direction of propagation of the wave, based on simplified models of the FAST, show that a turbulent flow field suddenly arises behind the shock. The closure of the boundary layer can lead to a fully turbulent flow behind the shock. Therefore viscosity could play an important role in the shock properties, affecting its strength as well as its speed of propagation. The interaction between the boundary layer and the shock is at present a topic on which a large number of researchers is working. Viscous unsteady simulations of the FAST are planned.